Contrib Mineral Petrol (2004) 148: 380–389
DOI 10.1007/s00410-004-0610-2

ORIGINAL PAPER

**Shyh-Lung Hwang · Pouyan Shen · Hao-Tsu Chu
Tzen-Fu Yui · Juhn G. Liou · Nikolay V. Sobolev
Ru-Yuan Zhang · Vladislav S. Shatsky
Anton A. Zayachkovsky**

# Kokchetavite: a new potassium-feldspar polymorph from the Kokchetav ultrahigh-pressure terrane

Received: 14 October 2003 / Accepted: 16 August 2004 / Published online: 14 September 2004


**Abstract** Kokchetavite, a new polymorph of K-feldspar ($KAlSi_3O_8$), has been identified as micrometer-size inclusions in clinopyroxene and garnet in a garnet-pyroxene rock from the Kokchetav ultrahigh-pressure terrane, Kazakhstan. Kokchetavite has a hexagonal structure with $a = 5.27(1)$ Å, $c = 7.82(1)$ Å, $V = 188.09$ Å$^3$, $Z = 1$, and is found to be associated with phengite + $\alpha/\beta$-cristobalite (or quartz) + siliceous glass ± phlogopite/titanite/calcite/zircon, occurring as multi-phase inclusions in clinopyroxene and garnet. It is concluded that kokchetavite could not be an exsolution phase in host minerals. Instead, it might be metastably precipitated from an infiltrated K-rich melt during rock exhumation. Alternatively, although less likely, kokchetavite might be derived from dehydration of K-cymrite, which, in turn, was formed at high pressures. In either case, kokchetavite is a metastable polymorph of K-feldspar.

Editorial Responsibility: W. Schreyer

S.-L. Hwang (✉)
Department of Materials Science and Engineering,
National Dong Hwa University,
Hualien, Taiwan, ROC
E-mail: slhwang@mail.ndhu.edu.tw

P. Shen
Institute of Materials Science and Engineering,
National Sun Yat-sen University,
Kaohsiung, Taiwan, ROC

H.-T. Chu
Central Geological Survey,
P.O. Box 968, Taipei,
Taiwan, ROC

T.-F. Yui
Institute of Earth Sciences,
Academia Sinica,
Taipei, Taiwan, ROC

J. G. Liou · R.-Y. Zhang
Department of Geological and
Environmental Sciences,
Stanford University,
Stanford, CA, 94305 USA

N. V. Sobolev · V. S. Shatsky
Institute of Mineralogy and Petrography,
Siberian Branch of Russian Academy of Sciences,
630090 Novosibirsk, Russia

A. A. Zayachkovsky
NEDRA Geological Expedition,
475013 Kokchetav, Kazakhstan

## Introduction

Potassium uptake in clinopyroxene has been observed in kimberlite, inclusions in diamond, and diamondiferous ultrahigh-pressure (UHP) rocks and is considered to be a potential barometer for very high-pressure rocks in the deep mantle (Bishop et al. 1978; Harlow and Davies 2004; Harlow and Veblen 1991; Katayama et al. 2002; Liou et al. 1998; Shatsky et al. 1995). In the past decade, K-rich (up to 1.6 wt%) clinopyroxene in diamondiferous UHP metamorphic rocks from the Kokchetav Massif has been intensively studied (Katayama et al. 2002; Perchuk et al. 2002, 2003; Sobolev and Shatsky 1990). This K-rich clinopyroxene was reported to contain variable $K_2O$ content and abundant lamellae/inclusions of quartz, K-feldspar, phengite and phlogopite based on conventional optical microscopy, infrared spectroscopy, and electron probe microanalysis techniques. The K-feldspar lamellae/inclusions, especially, were considered as exsolution/reaction products from a K-rich clinopyroxene precursor derived from mantle depths (Perchuk et al. 2002; Zhang et al. 1997).

K-feldspar occurs in three forms in nature, including sanidine (C2/m), orthoclase (C2/m), and microcline ($P\bar{1}$). While Al, Si atoms are disordered in sanidine, the difference between orthoclase and microcline is essentially one of scale in the microtextures, coupled with differences with Al, Si order (Deer et al. 1992). No other stable/metastable K-feldspar polymorphs have ever been

reported in nature. At high pressures, K-feldspar first breaks down to form a wadeite type phase at $P > 6$ GPa, and then transforms to a hollandite structure at P~9 GPa under anhydrous conditions (Yagi et al. 1994). Under high partial pressure of water, K- feldspar reacts to form a hydrated phase $KAlSi_3O_8 \cdot nH_2O$ (Davies and Harlow 2002; Fasshauer et al. 1997; Harlow and Davies 2004; Massonne 1995; Seki and Kennedy 1964; Thompson et al. 1998), hereinafter referred to as K-cymrite (Massonne 1995). Upon heating under atmospheric pressure, the water in K-cymrite could be completely removed to produce a metastable anhydrous, hexagonal $KAlSi_3O_8$ (Thompson et al. 1998). K-cymrite can exist over a broad range of temperatures at high pressures and has been considered important to water recycling or potassic interactions in the mantle (Davies and Harlow 2002). Although not yet found in nature, possible pseudomorph after K-cymrite consisting of K-feldspar + quartz + micaceous material or K-feldspar + quartz inclusion assemblages were reported and discussed in the literature (Massonne 2003; Massonne and Nasdala 2002; Song et al. 2003).

In the present study, by employing analytical electron microscopy (AEM), we found that some K-rich inclusions in Kokchetav UHP rocks, which might be easily misidentified as K-feldspar by the conventional techniques, are actually hexagonal $KAlSi_3O_8$. Since this is the first discovery of this phase in nature, we name it as Kokchetavite (IMA No. 2004-011), which has been approved by the Commission on New Minerals and Mineral Names (CNMMN) of the International Mineralogical Association (IMA).

## Geological background and sampling

The Kokchetav Massif is a large (300×150 km), fault-bounded metamorphic complex of Proterozoic protolith age in northern Kazakhstan. In the central part of this massif, seven tectonic melange units, resulting from collision between the Siberian platform and the Vendian-Ordovician island arc, have been collectively named as the Zerenda Series (Shatsky et al. 1995). The diamondiferous UHP rocks occur in unit I of the Zerenda Series, which consists of a variety of crystalline schist, gneiss, eclogite, amphibolite, garnet–pyroxene rocks, quartzite, marble and rare garnet peridotite. Abundant in-situ microdiamonds have been found as inclusions in garnet, zircon, and clinopyroxene in biotite gneiss, garnet–pyroxene rock and dolomite marble. Most of the protoliths of diamondiferous rocks were supracrustal rocks with a 2.2–2.3 Ga Sm–Nd model age (Shatsky et al. 1999). The peak metamorphic *P-T* conditions have been estimated around 5.8–6.5 GPa and 900–1,100°C. The age of the peak metamorphism has been determined around 530–540 Ma (see Parkinson et al. 2002).

The garnet–pyroxene rock sample KD-1 containing kokchetavite in the present study was collected from an underground mining gallery in Kumdy-Kol, Kazakhstan. The gallery had been constructed for microdiamond mining in 1981–1986 and was reconstructed in 2002. The lithologic characteristics of this mining gallery were well documented by previous investigators (Parkinson et al. 2002; Shatsky et al. 1995; Sobolev et al. 2003). Detailed geological map and section of Kumdy-Kol deposit including underground gallery were given by Sobolev et al. (2003). Briefly speaking, granitic gneiss, biotite gneiss and dolomite marble are the major rock types. Garnet–pyroxene rock occurs as layers up to 10 m thick within granitic and biotite gneisses (Shatsky et al. 1995). On the basis of geochemical characteristics, Shatsky et al. (1999) concluded that most Kokchetav UHP rocks might have been subjected to complicated partial melting processes yet to be studied.

## Analytical methods

Thin foils for AEM were prepared from petrographic thin sections. Clinopyroxene or garnet grains with inclusion pockets under optical microscope were first clamped between two copper rings to ensure sample integrity, followed by argon-ion-beam milling (Gatan, PIS) to perforation (operation condition: 4.0 kV, 9° incident angle). A carbon coat was applied to the specimens after ion thinning. Microstructure, mineralogy, and compositions of minerals were obtained using a transmission electron microscope (JEOL JEM-3010) operated at 300 kV. The transmission electron microscope was equipped with an energy dispersive X-ray (EDX) spectrometer (Oxford EDS-6636) with an ultra-thin window and a Si(Li) detector, capable of detection of elements from boron to uranium. The selective area electron diffraction (SAED) patterns were taken along various zone axes to determine the crystal system and the d-spacings. The d-spacings measured from SAED patterns and compiled in Table 2 were used for least-squares refinement of the lattice parameters of kokchetavite. The error of the d-spacing measurements on SAED patterns taken at a camera length of 150 cm and with cristobalite/quartz reflections as standard was estimated to be $\pm 0.02$ Å. Semi-quantitative chemical analysis was based on the Cliff-Lorimer thin film approximation with experimental k-factors obtained from natural minerals for K, Al, Na, Ca, Mg, Fe, and Ti (orthoclase, albite, diopside, Ti–clinohumite), and with factory preset k-factors (Link Virtual Standard Pack) for other elements (Lorretto 1994).

Raman spectra of kokchetavite were obtained from petrographic thin sections using a LABRAM HR confocal micro-Raman spectrometer equipped with Ar+ laser with 514.5 nm excitation. The laser beam size was about 2–4 μm and the laser power on the sampled surface was about 15 mW. The structural and compositional characteristics of kokchetavite were determined by the combined analyses of electron diffraction, EDX

analysis and Raman spectroscopy with characteristic bands assigned according to analogous mineral cymrite ($BaAl_2Si_2O_8{\cdot}H_2O$) (Graham et al. 1992).

## Experimental results

Polarized optical microscopy and electron microscopy coupled with EDX analysis indicate that garnet–pyroxene rock KD-1 consists predominantly of grossular-rich garnet ($Grs_{63}Adr_{12}Alm_{20}Prp_3Sps_2$) (~35% in mode) and pale green pleochroic clinopyroxene ($Di_{52}Hd_{48}$) (~60% in mode) with triple junctions characteristic of equilibrium recrystallization. Minor amounts (< 5% in mode) of K-feldspar, quartz and pyrrhotite ($Fe_{0.92}S$) occur along some grain boundaries of clinopyroxene and garnet (Fig. 1a). Whereas garnet grains have few inclusions, the clinopyroxene grains show cloudy cores full of micrometer- to submicrometer-size inclusions of various shapes lying subparallel to the parting of clinopyroxene (Fig. 1b). AEM further identified from clinopyroxene cores the following inclusion phases: Al-titanite (Al/Al + Ti ~ 0.4–0.5), talc + quartz, K-feldspar + quartz, fluid + vapor, and kokchetavite co-existing with $\alpha/\beta$-cristobalite, phengite, and a siliceous glass. Multiphase inclusions of kokchetavite + phengite + quartz ± siliceous glass ± phlogopite/titanite/calcite/zircon were also found in garnet grains. The morphological, chemical as well as structural characteristics of kokchetavite based on imaging, EDX analysis, electron diffraction, as well as Raman spectral analysis, of more than 20 independent observations (see Table 1), are described below.

Micrometer-size kokchetavite occurred predominantly as plates subparallel to the (100) parting of clinopyroxene, as indicated by aligned ones in neighboring inclusion pockets (3–7 μm in size) (Fig. 2a). Idiomor-

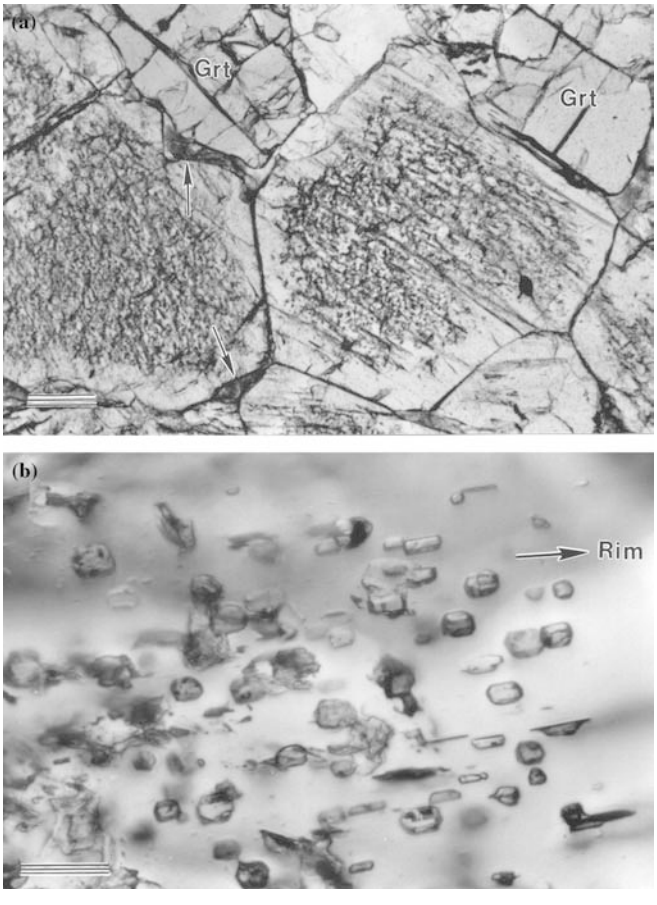


**Fig. 1** **a** Optical micrograph under plane polarized light of garnet (Grt)–clinopyroxene rock showing clinopyroxene grains with inclusion-free rim and inclusion-rich core. Inclusion pockets in clinopyroxene core are too tiny to be identified by optical properties. The intergranular K-feldspar and/or quartz are indicated by *arrows*. **b** Further magnified view of clinopyroxene grain showing inclusion-free rim and faceted inclusion pockets at core. Scale bars: $a = 200$ μm, $b = 25$ μm

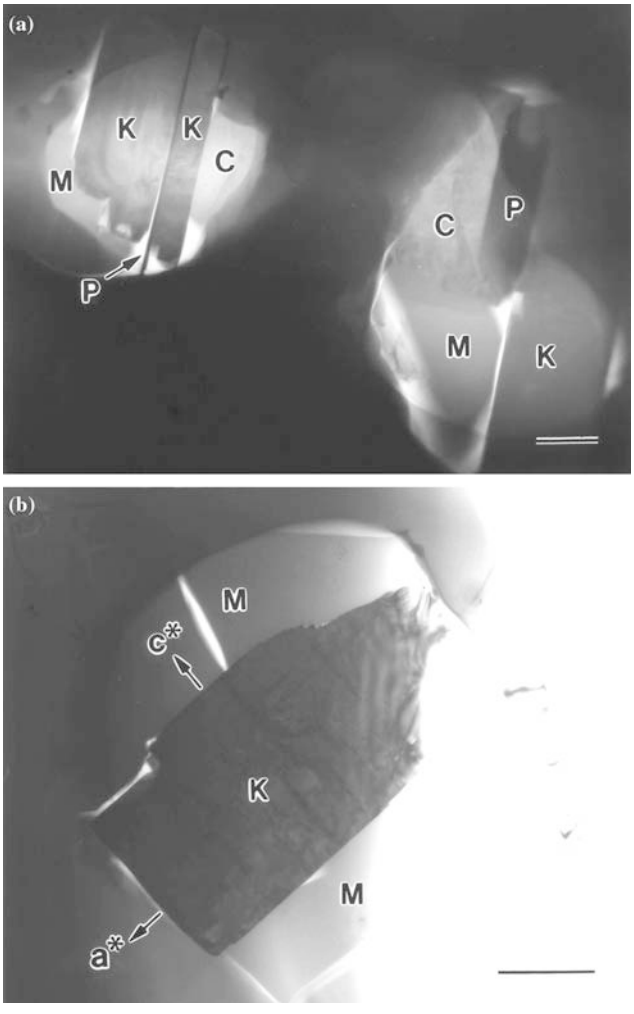


**Fig. 2** Transmission electron micrographs (*bright field images*) of kokchetavite (K) in association with other phases as inclusions in clinopyroxene host: **a** co-existing with siliceous glass (M) + $\alpha/\beta$-cristobalite (C) + phengite (P) in two neighboring inclusion pockets; **b** with growth steps (0001) and $\{10\bar{1}0\}$, perpendicular to $c^*$ and $a^*$ axes, respectively, adjoining siliceous glass M. Scale bars: *a*, *b* = 1 μm

phic prisms with random orientations and well-developed terraces and steps of (0001) and $\{10\bar{1}0\}$ planes were also observed (Fig. 2b).

Energy dispersive X-ray analysis indicated that the kokchetavite (Fig. 3a) contains 64.6–66.4% $SiO_2$, 18.0–18.9% $Al_2O_3$, and 15.5–16.8% $K_2O$ by weight. Trace of $Na_2O$ (<0.3%) was noted in a few analyses. (For comparison, EDX analysis of K-feldspar at grain boundary (Fig. 1a) or as inclusion in clinopyroxene was also performed, yielding 65.0–65.6% $SiO_2$, 17.7–18.7% $Al_2O_3$, and 15.6–16.4% $K_2O$, 0.5–0.7% $Na_2O$ by weight, typical of the K-feldspar compositions reported from Kokchetav UHP rocks (Sobolev and Shatsky 1990; Zhang et al. 1997).) These compositions are very close to the Si, Al, K stoichiometry of pure sanidine ($KAlSi_3O_8$), which is stable in the dry *P-T* condition of the mantle (Seki and Kennedy 1964). The associated phengite contains ~3.4–3.5 Si per formula unit. The quenched silica-rich melt (Fig. 3b) has compositions (75.1–79.4% $SiO_2$, 12.1–13.3% $Al_2O_3$, 4.1–6.2% $K_2O$, 2.5–4.2% CaO, 0.7–0.9% $Na_2O$, and trace of MgO (<0.3%) by weight.) similar to the composition of the melt phase at high *P-T* experiments (2.0–4.5 GPa and 850–1150°C) using a model composition pertinent to subducted crust in the $K_2O$–CaO–MgO–$Al_2O_3$–$SiO_2$–$H_2O$ system (denoted as KCMASH) (Hermann 2002; Hermann and Green 2001).

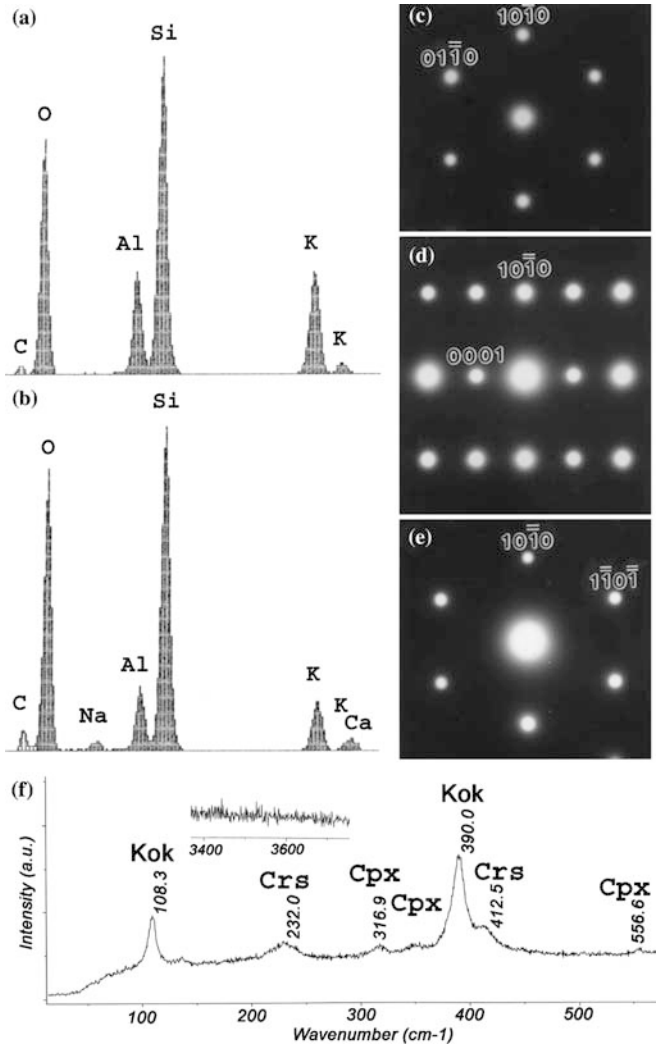


**Fig. 3** **a** and **b** Energy dispersive X-ray analysis of kokchetavite and siliceous glass, respectively. The carbon peaks were from carbon coating on TEM samples. **c–e** Selected area electron diffraction patterns of kokchetavite in the zone axes of [0001], $[1\bar{2}10]$, and $[1\bar{2}13]$, respectively. **f** Raman microprobe spectrum of kokchetavite (Kok) with additional peaks from cristobalite (Crs) and clinopyroxene (Cpx). The spectrum in the range of 3400–3700 $cm^{-1}$ in *inset* shows the absence of O–H stretching peak

The identity of kokchetavite was further verified by selected area electron diffraction patterns. The zone-axis patterns (Fig. 3c–e), the measured interplanar spacings, and the angles between zone axis patterns are all consistent with a hexagonal unit cell. The refined hexagonal lattice parameters $a = 5.27(1)$ Å and $c = 7.82(1)$ Å ($c/a = 1.484$, $V = 188.09$ Å$^3$, $Z = 1$, Table 2) are in close agreement with those of synthetic and dehydrated K-cymrite ($KAlSi_3O_8$) at room temperature and pressure ($a = 5.2893$ Å, $c = 7.8185$ Å) (Thompson et al. 1998) rather than the hydrated one ($KAlSi_3O_8 \cdot H_2O$ with $a = 5.3366$, $c = 7.7141$ Å or $a = 5.3348$, $c = 7.7057$ Å) (Table 3) (Fasshauer et al. 1997; Thompson et al. 1998). Hexacelsian ($BaAl_2Si_2O_8$) (Tabira et al. 2000; Takéuchi 1958), which is isostructural to K-cymrite, was also listed in Table 3 for comparison. Analogous to hexacelsian, there may be weak diffuse scatter intensity perpendicular to $\langle 11\bar{2}0 \rangle$ directions due to coupled tetrahedral rotation of $\langle 11\bar{2}0 \rangle$ columns of corner connected (Si, Al)$O_4$ tetrahedra. In addition, there are $G + 1/2\langle 1\bar{1}01 \rangle^*$ (*G*: fundamental spots) superlattice reflections due to a body-centered orthorhombic polymorph stable at low-temperatures (Tabira et al. 2000). All of these additional diffractions came from local domains of kokchetavite crystals. Because of its metastable nature, kokchetavite decomposed readily under a concentrated electron beam, and it was impossible to identify its point group, and hence space group using the convergent-beam electron-diffraction technique. However, a systematic absence of reflections was not observed in all SAED patterns, along with the similar crystal system, unit-cell parameters, cationic stoichiometry, as well as diffraction abnormalities mentioned above, indicating that kokchetavite likely belongs to the space group *P*6/*mmm*, as hexacelsian, synthetic K-cymrite, and probably dehydrated K-cymrite (Table 3).

The presence of Raman peaks at ~108 and ~391 $cm^{-1}$ (corresponding peaks for cymrite are at 104 and 396 $cm^{-1}$) (Fig. 3f) and the absence of characteristic peak of K-feldspar at ~514 $cm^{-1}$ are consistent with cymrite structure (Graham et al. 1992), not feldspar structure (Yang et al. 1998). The anhydrous nature was confirmed by the absence of O–H stretching peak in the range of 3,400–3,700 $cm^{-1}$. A constant $c/a$ ratio regardless of electron irradiation also confirms its anhydrous nature.

**Table 1** Mineral associations of inclusion pockets in clinopyroxene (Cpx) and garnet (Grt) in sample KD-1

| Host mineral | Pocket | Kok | Glass | Phn | Crs/qtz | Others |
|---|---|---|---|---|---|---|
| Cpx | A1 | X | – | – | – | – |
| | B1 | X | X | – | – | – |
| | C1 | X | X | – | – | – |
| | C2 | X | X | – | – | – |
| | E1 | X | X | – | X | – |
| | E2 | X | – | X | – | – |
| | E3 | X | X | – | X | – |
| | E4 | X | X | – | – | – |
| | F1 | X | X | X | – | – |
| | F2 | X | – | X | – | – |
| | H1 | X | X | – | – | – |
| | I1 | X | – | – | – | – |
| | I2 | X | – | – | X | – |
| | I3 | X | – | X | X | – |
| | I4 | X | X | – | – | – |
| | I5 | X | X | X | X | – |
| | I6 | X | X | X | X | – |
| | I7 | X | X | X | – | – |
| | I8 | X | X | – | – | – |
| Grt | G11 | X | – | X | X | – |
| | G21 | X | – | X | X | – |
| | G31 | X | X | X | X | Zrc |
| | G41 | X | – | – | X | Phl, Cal, titanite |

*Kok* kokchetavite, *Phn* phengite, *Crs* cristobalite, *Qtz* quartz, *Zrc* zircon, *Phl* phlogopite and *Cal* calciteX denotes the specific phase present

Similar inclusion pockets, although not as common as the case in clinopyroxene, were also found in garnet (Fig. 4a). Most of these inclusion pockets are about 2–5 μm in size and contain kokchetavite + phengite + quartz ± siliceous glass as represented by the TEM image in Fig. 4b. Trace tiny zircon crystals are surrounded by kokchetavite. The phengite has similar Si content (~3.5 Si per formula unit) as that in the inclusion pockets in clinopyroxene. Inclusion pocket larger than 10 μm in size with multiple phases of kokchetavite + quartz + phlogopite + titanite + calcite was occasionally found in garnet. Well-developed terraces and steps of (0001) and $\{10\bar{1}0\}$ planes were also observed for kokchetavite when adjoined with siliceous glass in garnet.

Many kokchetavite inclusions have preferred orientation but not necessarily in exact epitaxy with the clinopyroxene host. Under such a circumstance, the c* of kokchetavite tends to be subparallel (a few degrees off) to a* of clinopyroxene. However, randomly oriented kokchetavite was frequently found (4 of 19 inclusion pockets) in clinopyroxene hosts. By contrast, all kokchetavite inclusions are in random orientation within the garnet host. When associated with phengite in both clinopyroxene and garnet, topotaxy matching the identical basal layers of linked (Si, Al)$O_4$ tetrahedra in phengite and kokchetavite was observed: $(001)_{Phn}//(0001)_{Kok}$ and $[010]_{Phn}//[1\bar{1}00]_{Kok}$.

**Table 2** d-spacings (Å) and lattice parameters (Å) of kokchetavite

| hkl | Observed[a] | Calculated[b] | Refined[a] |
|---|---|---|---|
| 001 | 7.82 | 7.82 | 7.82 |
| 100 | 4.56 | 4.58 | 4.56 |
| 101 | 3.93 | 3.95 | 3.94 |
| 102 | 2.98 | 2.97 | 2.97 |
| 110 | 2.63 | 2.65 | 2.63 |
| 111 | 2.51 | 2.51 | 2.50 |
| 103 | 2.26 | 2.27 | 2.26 |
| 104 | 1.80 | 1.80 | 1.80 |
| 210 | 1.72 | 1.73 | 1.72 |
| 211 | 1.68 | 1.69 | 1.68 |

[a]Kokchetavite: $a = 5.27 \pm 0.01$ Å, $c = 7.82 \pm 0.01$ Å
[b]Dehydrated synthetic K-cymrite: $a = 5.2893 \pm 0.0016$ Å, $c = 7.8185 \pm 0.0036$ Å (after Thompson et al. 1998)

## Discussion

### Formation of kokchetavite

The common occurrence of kokchetavite in the multiple phase inclusions in clinopyroxene and garnet of the garnet–pyroxene rock is significant. These kokchetavite crystals could be a result of (1) solid-state exsolution during decompression of the K-rich host minerals similar to that proposed to explain the occurrences of K-feldspar/phlogopite lamellae in clinopyroxene from UHP rocks (Zhang et al. 1997), (2) dehydration of K-cymrite which, in turn, was a high-pressure precipitate from a precursor K-rich melt intruding into the host grains along open cleavages/partings, or (3) non-equilibrium precipitation from a precursor K-rich melt during exhumation.

#### *Solid-state exsolution in K-rich host minerals during exhumation*

Exsolution microstructures have been found in ultrahigh-pressure ultramafic and eclogitic rocks of orogenic belts worldwide. Typical examples include ilmenite rods and magnetite plates in olivine; K-feldspar, phlogopite, Mg–Al–Cr titanomagnetite and/or ilmenite, quartz, and garnet rods in clinopyroxene; pyroxene and rutile lamellae in garnet; monazite lamellae in apatite; and coesite in titanite (Ogasawara et al. 2002; Zhang and Liou 1999 and references cited therein). In most cases, the apparent alignment of inclusions under optical microscope or scanning electron microscope was taken as evidence for their exsolution origin, resulting from the nearly isothermal decompression of the very high-pressure precursor phases.

To reduce nucleation/growth barrier, coherent interfaces are usually preserved when solutes exsolve from an oversaturated matrix (Putnis 1992). Excellent crystallographic relations between hosts and precipitates have usually been observed, such as ilmenite rods/magnetite plates in olivine, rutile needles in gar-

**Table 3** Structure comparison between kokchetavite, hexacelsian, dehydrated synthetic K-cymrite, and synthetic K-cymrite

| | Kokchetavite | Hexacelsian[a] | Dehydrated K-cymrite[b] | K-cymrite[b, c] |
|---|---|---|---|---|
| System | Hexagonal | Hexagonal | Hexagonal | Hexagonal |
| *a* (Å) | 5.27 | 5.31 | 5.29 | 5.34 |
| *c* (Å) | 7.82 | 7.81 | 7.82 | 7.71 |
| Space group | *P6/mmm?* | *P6/mmm* | *P6/mmm?* | *P6/mmm* |

[a]Takéuchi (1958),
[b]Thompson et al. (1998),
[c]Fasshauer et al. (1997)

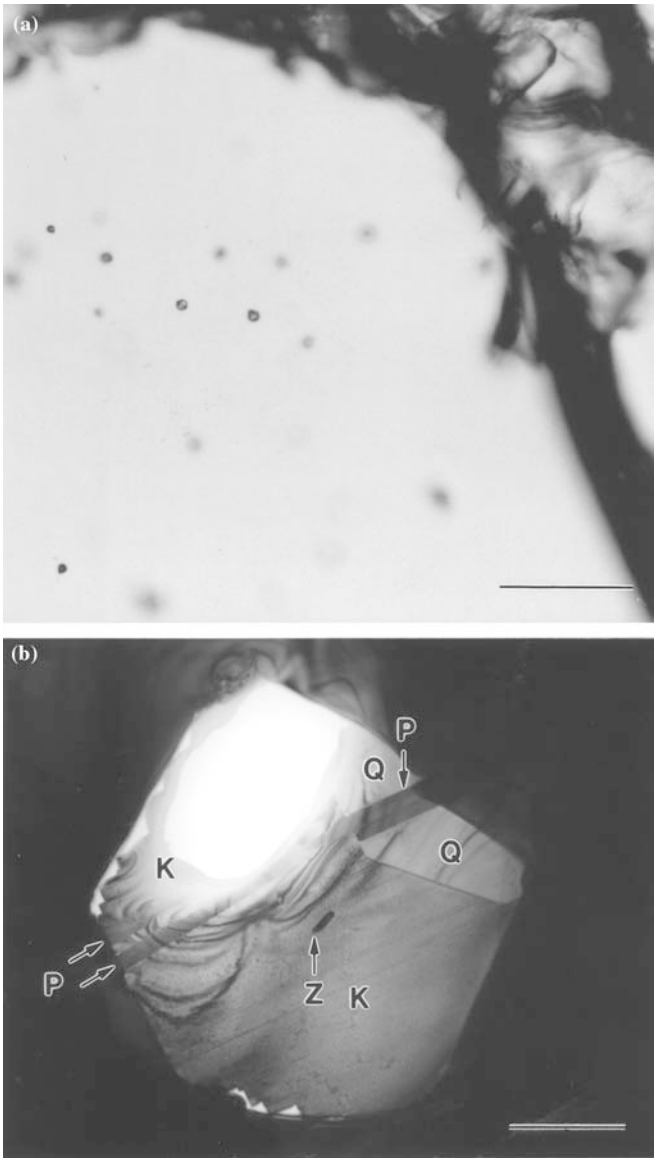


**Fig. 4** **a** Optical micrograph under plane polarized light of garnet (Grt) in KD-1 sample showing composite inclusion pockets in garnet host too tiny to be identified by optical properties. **b** Representative transmission electron micrograph (bright field images) of kokchetavite (K) and zircon (Z) in association with other phases [α-quartz (Q) + phengite (P)] as inclusions in garnet host. Scale bars: $a = 50$ μm, $b = 1$ μm

net and in corundum, Fe-rich precipitates in iron-bearing rutile, as well as numerous other examples (Hacker et al. 1997; Putnis 1992; Zhang et al. 2003, 2004). The observed kokchetavite crystals, however, are not in epitaxial relationships with clinopyroxene host; in fact, they can even be randomly oriented within the hosting garnet, according to the detailed electron diffraction study described above. These observations obviously do not support an exsolution origin of kokchetavite. Moreover, the co-existence of kokchetavite together with phengite, silica, and residue glass phase in a single inclusion pocket, as well as the common occurrence of inclusion pockets with nearly identical multiple-phase assemblages in two host minerals (diopside and garnet) of very different crystal nature (i.e. chain silicate vs. orthosilicate), do not support any known exsolution mechanism. Instead, the common inclusion pockets with similar phase assemblages in both clinopyroxene and garnet implies a foreign source, i.e. a precursor melt, for kokchetavite as discussed later.

### *Dehydration of high-pressure K-cymrite*

In light of the observation that, instead of becoming stable K-feldspar, synthetic K-cymrite dehydrated as a hexagonal $KAlSi_3O_8$ phase (probably isostructural to kokchetavite) at $T > 300$°C at ambient pressure (Thompson et al. 1998), the present kokchetavite could originate from the dehydration of a precursor K-cymrite. Experimentally, K-cymrite has been found to form in hydrothermal treatment of either sanidine or gel of sanidine composition (Fasshauer et al. 1997; Massonne 1995; Seki and Kennedy 1964; Thompson et al. 1998). In these experiments with excess $H_2O$, the phase boundary for K-feldspar + $H_2O$ = K-cymrite intersects the K-cymrite + coesite + $H_2O$ melting curve at $T = 704$°C, $P = 2.70$ GPa for $a_{H_2O} = 1$ (Fig. 5) (Fasshauer et al. 1997; Huang and Wyllie 1975; Thompson et al. 1998). The phase boundaries for these two reactions move, respectively, to higher P or T with decreasing water activity, as shown in the K-feldspar + $H_2O$ = K-cymrite phase boundary for $a_{H_2O} = 0.5$ and 0.1 (Fig. 5) (Fasshauer et al. 1997). Therefore, with decreasing water

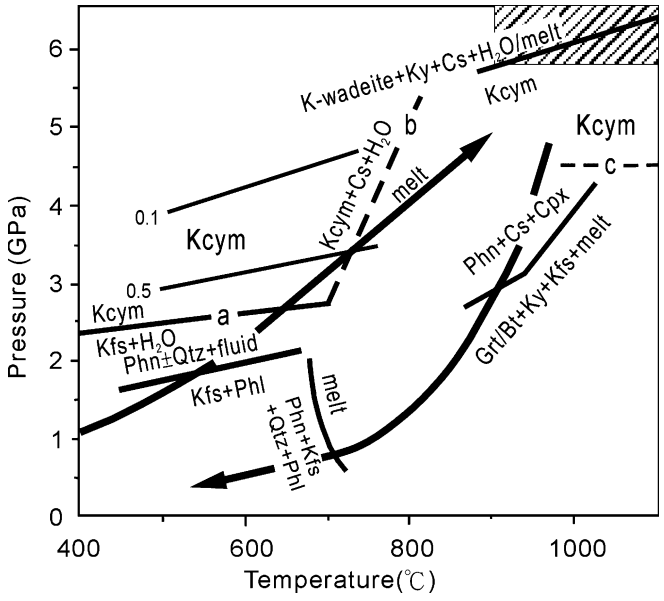


**Fig. 5** Generalized *P-T* path (Katayama et al. 2000; Katayama et al. 2001) and peak *P-T* conditions (hatched box) (Parkinson et al. 2002) of diamondiferous Kokchetav Massif. Also shown are the K-cymrite (Kcym)/K-feldspar (Kfs) phase boundaries: Kfs + $H_2O$ = Kcym curve at specified $a_{H_2O}$ of 1 (*curve a*), 0.5 and 0.1 (Fasshauer et al. 1997; Thompson et al. 1998); Kcym melting curves in the presence of excess $H_2O$ and $SiO_2$ (*curve b*) (Huang and Wyllie 1975); phengite (Phn)-in curve in the KMASH system: Kfs + phlogopite (Phl) = Phn ± Qtz + fluid (with oversaturated $H_2O$ and $SiO_2$) (Massonne 1992); melting curve in the KMASH system: Phn + Kfs + Qtz + Phl = melt (Massonne and Schreyer 1987); Phn-out melting curve in the KCMASH system: Phn + coesite (Cs) + clinopyroxene = garnet + kyanite (Ky) + Kfs + melt or biotite + Ky + Kfs + melt (Hermann 2002; Hermann and Green 2001); formation of K-cymrite (*curve c*) and Kcym = K-wadeite + Ky + Cs + melt or $H_2O$ (Davies and Harlow 2002)

activity, the stability field of K-cymrite moves to higher temperatures and pressures. Alternatively, in the experiments starting with equimolar $H_2O$ + either gel ($Or_{97}Qtz_3$) or natural sanidine ($Or_{97}Ab_3$), K-cymrite was found to be stable in assemblages of either K-cymrite + silica + melt or K-cymrite + jadeite + melt at 4.5 GPa and 1,000–1,300°C (Fig. 5, *P-T* ranges above curve c) (Davies and Harlow 2002; Harlow and Davies 2004). K-cymrite is stable up to 6 GPa and 1,000°C, at which it breaks down to K-wadeite + kyanite + silica + $H_2O$ (Davies and Harlow 2002; Harlow and Davies 2004). Under such *P-T* conditions, K-cymrite formation was found to be highly dependent upon initial water contents in the experimental charges, and experiments containing more than equimolar $H_2O$ produced sanidine plus melt (R. Davies 2003, personal communication). According to these experiments, K-cymrite could form under broad *P-T* ranges covering parts of the prograde/retrograde paths and the peak conditions of Kokchetav UHP rocks.

Along the prograde path of Kokchetav rocks (Katayama et al. 2000), the breakdown reaction of K-feldspar + phlogopite would form phengite + K, Mg-rich siliceous fluid above 1.5 GPa at 400–700°C (Fig. 5) in the $SiO_2$- and $H_2O$-saturated KMASH system (Massonne 1992). This K, Mg-rich siliceous fluid may contain < 15 wt% $H_2O$ and is probably supercritical with the character of a silicate melt (Massonne 1992). The K-cymrite would probably crystallize from this K, Mg-rich siliceous fluid after entrapment within clinopyroxene/garnet at high pressures (Fig. 5) and dehydrate to form kokchetavite under dry mantle conditions. In this case, the released water must either be uptaken by clinopyroxene/garnet hosts as structural water (Ingrin and Skogby 2000 and references cited therein), or diffuse out of the hosts into the environment. Although the experimental data showed the fast hydrogenation–dehydrogenation kinetics of diopside and iron-rich pyrope at $T$ = 700–1,000°C (Hercule and Ingrin 1999; Ingrin and Skogby 2000; Wang et al. 1996), it is still a little bit difficult to envisage the preservation of metastable kokchetavite, instead of transformation into K-feldspar, before the dehydrated water was uptaken by or diffused out of the host minerals. This consideration renders the formation of kokchetavite through dehydration of a precursor K-cymrite less likely.

### *Non-equilibrium precipitation of kokchetavite during exhumation*

Cymrite ($BaAl_2Si_2O_8{\cdot}H_2O$), a structural analogue of K-cymrite (Fasshauer et al. 1997; Massonne 1995; Seki and Kennedy 1964; Thompson et al. 1998), has been identified in rocks subjected to low-temperature, high-pressure metamorphism (Hsu 1994; Reinecke 1982). The equilibrium phase boundary between cymrite and celsian ($BaAl_2Si_2O_8$) has been experimentally determined to be located at 6 kbar and 300°C, as well as 9 kbar and 900°C with a positive *P-T* slope (Graham et al. 1992). At pressures below the equilibrium boundary, an 'intermediate' cymrite ($BaAl_2Si_2O_8{\cdot}nH_2O$, $0 < n < 1$) with intermediate water contents crystallized metastably in hydrothermal experiments at temperatures below 600°C and pressures of 1–3 kbar (Graham et al. 1992; Viswanathan et al. 1992). On the other hand, hexacelsian (hexagonal $BaAl_2Si_2O_8$, stable above 1,590°C) could metastably form in the stability field of celsian in dry experiments, yet converts to celsian at T = 393–1,585°C when $H_2O$ vapor is present (Lin and Foster 1968). Similar to intermediate cymrite and hexacelsian, the present kokchetavite could also have formed metastably in the stability field of ordinary K-feldspar during exhumation.

The exhumation path of Kokchetav rocks crosses the solidus of phengite-bearing pelitic country rocks in the KCMASH system (Hermann 2002; Hermann and Green 2001; Katayama et al. 2001) at the *P-T* conditions inside the stability field of sanidine (Fig. 5). Thus, thermodynamically, kokchetavite would not crystallize from such infiltrated melts during rock exhumation. Although metastable kokchetavite could have formed from a glass in the presence of catalytic nuclei likely provided by

precursor infiltrated melts, the well-developed growth terraces and steps rather than dendrites for the kokchetavite crystals suggest that they would have most probably precipitated/grown from a melt phase. The apparent textural equilibrium among coexisting phases in the inclusion pockets (Fig. 2) also supports this scenario. It was noted that when kokchetavite was associated with phengite in inclusion pockets from both clinopyroxene and garnet, there was an excellent topotaxy matching of the linked (Si, Al)$O_4$ hexagonal basal layers of similar dimensions between kokchetavite (i.e., 5.27 Å) and phengite (i.e., 5.23 Å). A coherent/semicoherent interface would reduce interfacial energy and hence lower the activation energy for heterogeneous nucleation of kokchetavite on top of phengite basal layer. This could possibly lead to the metastable formation of kokchetavite within the stability field of sanidine. Alternatively, the metastable formation of kokchetavite could be due to surface energy and hence size effects, similar to the metastable occurrence of boemite/gibbsite in the stability field of diaspore, or the moganite in the stability field of quartz (Majzlan et al. 2000; Petrovic et al. 1996). A K-rich melt entrapped along the partings/cleavages of clinopyroxene/garnet may account for the non-equilibrium precipitation of kokchetavite during uplift. When the retrograde path approached the melting curve of the assemblage: phengite + K-feldspar + quartz + phlogopite in the KMASH system (Massonne and Schreyer 1987) (Fig. 5), the entrapped K-rich melt could crystallize phengite + kokchetavite + silica with a residue melt. The absence of phlogopite in most of the inclusion pockets apparently was due to the low MgO content in the melt. After formation, kokchetavite persisted to the ambient condition because of the sluggish transformation to stable sanidine at low temperatures involving bond breaking and rearrangement of atoms (Putnis 1992).

The scenario of metastable formation of kokchetavite seems reasonable, but not without difficulties. First, not all kokchetavite-bearing pockets contain phengite. Second, unlike the cymrite-celsian system, K-feldspar related metastable phases have not been synthesized. (Only a small number of experiments have been performed.) Lastly, the inclusion-free rim of clinopyroxene (Fig. 1a) would have formed during the retrograde stage in this scenario, although there are no prominent chemical differences between clinopyroxene core and rim.

One more thing should be pointed out is that the garnet–pyroxene rock in the present study is poor in K and might not be able to produce the proposed K-rich melt through partial melting. Although it cannot be ruled out that the K-rich melts responsible for the formation of kokchetavite in the present study has a mantle origin as suggested by Perchuk et al. (2002, 2003) and Zhu (2003), partial melting of the surrounding gneissic rocks, which contain diamond/graphite + coesite/quartz + garnet + clinopyroxene + phengite + plagioclase + K-feldspar + aragonite/calcite + amphibole + chlorite ± phlogopite/biotite ± zoisite ± rutile, would be a more reasonable source for the infiltrated melts considering the structurally coherent nature of the present UHP rocks. In either case, K would be derived externally since garnet, one of the hosting minerals of kokchetavite, can hardly accommodate K in its lattice sites.

## Formation of cristobalite/glass

The $\alpha/\beta$-cristobalite phases randomly orientated with respect to clinopyroxene host are not stable along the *P-T* path shown in Fig. 5. They could have formed by metastable crystallization from siliceous melt at low temperatures. The metastable occurrence of cristobalite may be due to the influence of minor contents of impurities such as $Al^{3+}$, $Ca^{2+}$, $Mg^{2+}$, and $Na^{+}$ (Thomas et al. 1994). A valid stabilization of cristobalite with minor amounts of impurities for the present UHP sample may also rely on specific *P-T* path and volume misfit with respect to the host, analogous to the retention of cristobalite inclusions in the garnets of Gore Mountain, which was suggested to have metastably precipitated from a hydrous Na–Al siliceous melt (Darling et al. 1997).

Rather than amorphization of a precursor crystalline phase by argon ion milling and/or electron dosage, the siliceous glass with Al, K, Na and Ca ions was derived from a former melt that was quickly chilled to result in the observed structural state. This interpretation is in accord with glass-forming compositions in the quaternary systems $K_2O$–$Al_2O_3$–CaO–$SiO_2$ and $Na_2O$–$Al_2O_3$–CaO–$SiO_2$ (Kingery et al. 1983; Vogel 1985) and the occurrence of Na–Al silicate glass of primary origin in association with diamond-bearing inclusion pockets in garnet of UHP rocks from Erzgebirge, Germany (Hwang et al. 2001).

## Concluding remarks

In essence, we have identified numerous kokchetavite inclusions in clinopyroxene and garnet from Kokchetav UHP garnet–pyroxene rocks. It is clearly demonstrated that kokchetavite could no be an exsolution phase from the hosting minerals. It is postulated that kokchetavite may have metastably crystallized from (infiltrated) melts during retrograde exhumation. Alternatively, but less likely, kokchetavite may have been formed from the dehydration of K-cymrite which, in turn, was a high-pressure precipitate from (infiltrated) melts. Whether kokchetavite has ever been subjected to retrograde fluid infiltration/entrapment to form inclusions of talc + -quartz and K-feldspar + quartz, is not certain. The external source of the melts and the possible interactions between included melt and host minerals are yet to be evaluated.

By conventional techniques, some lamellae/inclusions in clinopyroxene of UHP rocks have been suggested to be K-feldspar, which was postulated to be exsolution/

reaction products from a K-rich clinopyroxene precursor. The precursor's K content was therefore recalculated based on the modal composition of lamellae/inclusions and was employed to infer the pressure condition of the precursor clinopyroxene (Perchuk et al. 2002, 2003; Zhang et al. 1997; Zhu 2003). The present study, through AEM observations, clearly shows that some of the K-feldspars in the previous studies might actually be kokchetavite, which was most likely derived from a K-rich melt of external origin. The modal abundance of this phase should therefore be related to the prevalence of channel ways in hosting minerals for melt infiltration and have nothing to do with the K content of precursor clinopyroxene. Its modal abundance therefore should not be employed to estimate the pressure condition of the hosting rock.

Based on experimental work, K-cymrite, with a zeolite-like structure, has been considered to be an important water-bearing phase in deep subducted crustal rocks (Davies and Harlow 2002; Fasshauer et al. 1997; Massonne 1995; Thompson et al. 1998). Despite its possible role in potassium and water recycling, the natural occurrence of K-cymrite has never been proved (Massonne 2003; Massonne and Nasdala 2002; Song et al. 2003). In the present study, kokchetavite and K-feldspar are common inclusion phases in clinopyroxene and garnet in Kokchetav UHP garnet–pyroxene rocks. This may imply that even if K-cymrite did form during subduction of crustal rocks, the phase may have easily transformed to kokchetavite/K-feldspar and hardly be preserved during rock exhumation.

The calculated density of kokchetavite is 2.45 g/cm$^3$ based on the chemical formula and lattice parameters determined in this work. This value is close to that of dehydrated synthetic K-cymrite (2.44 g/cm$^3$) at ambient conditions, but is significantly different from that of sanidine (2.56–2.62 g/cm$^3$). This supports the metastability of kokchetavite discussed in the text just like the appearance of cristobalite in the inclusions.

Holotype material of kokchetavite, a thin rock slab of sample KD-1, is housed in the National Museum of Natural Science, Taichung, Taiwan, under accession number NMNS004438-P010220.

**Acknowledgments** We thank Y.C. Yang for the expertise on the Raman microprobe, L.J. Wang for technical assistance on AEM, and Jacob Chu for reading the manuscript. Helpful suggestions from W.G. Ernst, R. Davies, H.J. Massonne, E.A.J. Burke, and W. Schreyer are greatly appreciated. This research was supported by National Science Council, Taiwan, ROC (S.-L.H., P.S., H.-T.C., T.-F.Y.) and also in part by a Civilian Research Development grant (RG1-2387-NO-02) through a US–Russian–Taiwan cooperative project.

## References

Bishop FC, Smith JV, Dawson JB (1978) Na, K, P and Ti in garnet, pyroxene and olivine from peridotite and eclogite xenoliths from African kimberlites. Lithos 11:155–173

Darling RS, Chou IM, Bodnar RJ (1997) An occurrence of metastable cristobalite in high-pressure garnet granulite. Science 276:91–93

Davies R, Harlow GE (2002) The high pressure stability of K-cymrite and phases in the system Or–$H_2O$. Eos Transaction AGU, vol 83, no. 47. Fall Meet Suppl Abstr, V72B-1308

Deer WA, Howie RA, Zussman J (1992) The rock-forming minerals. Longman Scientific & Technical, England, p 696

Fasshauer DW, Chatterjee ND, Marler B (1997) Synthesis, structure, thermodynamic properties, and stability relations of K-cymrite, $K[AlSi_3O_8]\cdot H_2O$. Phys Chem Minerals 24:455–462

Graham CM, Tareen JAK, McMillan PF, Lowe BM (1992) An experimental and thermodynamic study of cymrite and celsian stability in the system BaO–$Al_2O_3$–$SiO_2$–$H_2O$. Eur J Mineral 4:251–269

Hacker BR, Sharp T, Zhang RY, Liou JG, Hervig RL (1997) Determining the origin of ultrahigh-pressure lherzolites. Science 278:702–704

Harlow GE, Davies R (2004) Status report on stability of K-rich phases at upper-mantle conditions. Lithos (in press)

Harlow GE, Veblen DR (1991) Potassium in clinopyroxene inclusions from diamonds. Science 251:652–655

Hercule S, Ingrin J (1999) Hydrogen in diopside: diffusion, extraction-incorporation, and solubility. Am Mineral 84:1577–1588

Hermann J (2002) Experimental constraints on phase relations in subducted continental crust. Contrib Mineral Petrol 143:219–235

Hermann J, Green DH (2001) Experimental constraints on high pressure melting in subducted crust. Earth Planet Sci Lett 188:149–168

Hsu LC (1994) Cymrite: new occurrence and stability. Contrib Mineral Petrol 118:314–320

Huang WL, Wyllie PJ (1975) Melting reactions in the system Na-$AlSi_3O_8$–$KAlSi_3O_8$–$SiO_2$ to 35 kbar, dry and with excess water. J Geol 83:737–748

Hwang SL, Shen P, Chu HT, Yui TF, Lin CC (2001) Genesis of microdiamonds from melt and associated multiphase inclusions in garnet of ultrahigh-pressure gneiss from Erzgebirge, Germany. Earth Planet Sci Lett 188:9–15

Ingrin J, Skogby H (2000) Hydrogen in nominally anhydrous upper-mantle minerals: concentration levels and implications. Eur J Mineral 12:543–570

Katayama I, Zayachkovsky AA, Maruyama S (2000) Prograde pressure-temperature records from inclusions in zircons from ultrahigh-pressure-high-pressure rocks of the Kokchetav Massif, northern Kazakhstan. The Island Arc 9:417–427

Katayama I, Maruyama S, Parkinson CD, Terada K, Sano Y (2001) Ion micro-probe U–Pb zircon geochronology of peak and retrograde stages of ultrahigh-pressure metamorphic rocks from the Kokchetav massif, northern Kazakhstan. Earth Planet Sci Lett 188:185–198

Katayama I, Ohta M, Ogasawara Y (2002) Phengite exsolution in diopside in diamond-bearing marble from Kumdy-Kol. In: Parkinson CD, Katayama I, Liou JG, Maruyama S (eds) The diamond-bearing Kokchetav Massif, Kazakhstan. Universal Academy Press Inc., Tokyo, pp 181–188

Kingery WD, Vandiver PB, Huang IW, Chiang YM (1983) Liquid–liquid immiscibility and phase separation in the quaternary systems $K_2O$–$Al_2O_3$–CaO–$SiO_2$ and $Na_2O$–$Al_2O_3$–CaO–$SiO_2$. J Noncryst Solids 54:163–171

Lin HC, Foster WR (1968) Studies in the system BaO–$Al_2O_3$–$SiO_2$ I. The polymorphism of celsian. Am Mineral 53:134–144

Liou JG, Zhang RY, Ernst WG, Rumble D, Maruyama S (1998) High-pressure minerals from deeply subducted metamorphic rocks. In: Hemley RJ (ed) Ultrahigh-pressure mineralogy: physics and chemistry of the earth's deep interior (Reviews in mineralogy, vol 37). Mineral. Soc. America, Washington, pp 33–96

Lorretto MH (1994) Electron beam analysis of materials, 2nd edn. Chapman & Hall, London, p 272

Majzlan J, Navrotsky A, Casey WH (2000) Surface enthalpy of boemite. Clays Clay Miner 48:699–707

Massonne HJ (1992) Evidence for low-temperature ultrapotassic siliceous fluids in subduction zone environments from experiments in the system $K_2O$–MgO–$Al_2O_3$–$SiO_2$–$H_2O$ (KMASH). Lithos 28: 421–434

Massonne HJ (1995) Experimental and petrogenetic study of UHPM. In: Coleman RG, Wang X (eds) Ultrahigh-pressure metamorphism. Cambridge University Press, Cambridge, pp 33–95

Massonne HJ (2003) A comparison of the evolution of diamondiferous quartz-rich rocks from the Saxonian Erzgebirge and the Kokchetav Massif: are so-called diamondiferous gneisses magmatic rocks?. Earth Planet Sci Lett 216:347–364

Massonne HJ, Nasdala L (2002) Characterization of an early metamorphic stage through inclusions in zircon of a diamondiferous quartzofeldspathic rock from the Erzgebirge, Germany. Am Mineral 88: 883–889

Massonne HJ, Schreyer W (1987) Phengite geobarometry based on the limiting assemblage with K-feldspar, phlogopite, and quartz. Contrib Mineral Petrol 96:212–224

Ogasawara Y, Fukasawa K, Maruyama S (2002) Coesite exsolution from supersilicic titanite in UHP marble from the Kokchetav Massif, north Kazakhstan. Am Mineral 87:454–461

Parkinson CD, Maruyama S, Liou JG, Kohn MJ (2002) Probable prevalence of coesite-stable metamorphism in collisional orogens and a reinterpretation of Barrovian metamorphism. In: Parkinson CD, Katayama I, Liou JG, Maruyama S (eds) The diamond-bearing Kokchetav Massif, Kazakhstan. Universal Academy Press Inc., Tokyo, pp 447–461

Perchuk LL, Safonov OG, Yapaskurt VO, Barton JM Jr (2002) Crystal-melt equilibria involving potassium-bearing clinopyroxene as indicator of mantle-derived ultrahigh-potassic liquid: an analytical review. Lithos 60:89–111

Perchuk LL, Safonov OG, Yapaskurt VO, Barton JM Jr (2003) Reply to comments by Y. Zhu: K-feldspar in clinopyroxene from Grt–Cpx silicate rocks of the Kokchetav Massif. Lithos 68:121–130

Petrovic I, Heaney PJ, Navrotsky A (1996) Thermochemistry of the new silica polymorph moganite. Phys Chem Minerals 23:119–126

Putnis A (1992) Introduction to mineral sciences. Cambridge University Press, Cambridge, p 457

Reinecke T (1982) Cymrite and celsian in manganese-rich metamorphic rocks from Andros island, Greece. Contrib Mineral Petrol 79:333–336

Seki Y, Kennedy GC (1964) The breakdown of potassium feldspar, $KAlSi_3O_8$, at high temperatures and high pressures. Am Mineral 49:1688–1706

Shatsky VS, Sobolev NV, Vavilov MA (1995) Diamond-bearing metamorphic rocks of the Kokchetav massif (northern Kazakhstan). In: Coleman RG, Wang X (eds) Ultrahigh-pressure metamorphism. Cambridge University Press, Cambridge, pp 427–455

Shatsky VS, Jagoutz E, Sobolev NV, Kozmenko OA, Parkhomenko VS, Troesch M (1999) Geochemistry and age of ultrahigh pressure metamorphic rocks from the Kokchetav massif (Northern Kazakhstan). Contrib Mineral Petrol 137:185–205

Sobolev NV, Shatsky VS (1990) Diamond inclusions in garnets from metamorphic rocks. Nature 343:742–746

Sobolev NV, Shatsky VS, Liou JG, Zhang RY, Hwang SL, Shen P, Chu HT, Yui TF, Zayachkovsky AA, Kasymov MA (2003) US-Russian civilian Research and Development Fund Project: an origin of microdiamonds in metamorphic rocks of the Kokchetav massif, northern Kazakhstan. Episodes 26:290–294

Song SG, Yang JS, Xu ZQ, Liou JG, Shi RD (2003) Metamorphic evolution of the coesite-bearing ultrahigh-pressure terrane in the North Qaidam, Northern Tibet, NW China. J Metamorphic Geol 21:631–644

Tabira Y, Withers RL, Takéuchi Y, Marumo F (2000) Structured diffuse scattering, displacive flexibility and polymorphism in Ba-hexacelsian. Phys Chem Minerals 27:194–202

Takéuchi Y (1958) A detailed investigation of the structure of hexagonal $BaAl_2Si_2O_8$ with reference to it's $\alpha$–$\beta$ inversion. Mineral J 2:311–332

Thomas ES, Thompson JG, Withers RL, Sterns M, Xiao Y, Kirkpatrick RJ (1994) Further investigation of the stabilization of $\beta$-cristobalite. J Am Ceram Soc 77:49–56

Thompson P, Parsons I, Graham CM, Jackson B (1998) The breakdown of potassium feldspar at high water pressures. Contrib Mineral Petrol 130:176–186

Viswanathan K, Harneit O, Epple M (1992) Hydrated barium aluminosilicates, $BaAl_2Si_2O_8{\cdot}nH_2O$, and their relations to cymrite and hexacelsian. Eur J Mineral 4:271–278

Vogel W (1985) Chemistry of glass. The American Ceramic Society, Columbus, Ohio, p 325

Wang L, Zhang Y, Essene EJ (1996) Diffusion of the hydrous component in pyrope. Am Mineral 81:706–718

Yagi A, Suzuki T, Akaogi M (1994) High pressure transition in the system $KAlSi_3O_8$–$NaAlSi_3O_8$. Phys Chem Minerals 21:12–17

Yang J, Godard G, Smith DC (1998) K-feldspar-bearing coesite pseudomorphs in an eclogite from Lanshantou (Eastern China). Eur J Mineral 10:969–985

Zhang RY, Liou JG (1999) Exsolution lamellae in minerals from ultrahigh-pressure rocks. Int Geol Rev 41:981–993

Zhang RY, Liou JG, Ernst WG, Coleman RG, Sobolev NV, Shatsky VS (1997) Metamorphic evolution of diamond-bearing and associated rocks from the Kokchetav Massif, northern Kazakhstan. J Metamorphic Geol 15:479–496

Zhang RY, Zhai SM, Fei YW, Liou JG (2003) Titanium solubility in coexisting garnet and clinopyroxene at very high pressure: the significance of exsolved rutile in garnet. Earth Planet Sci Lett 216: 591–601

Zhang RY, Liou JG, Zheng JP (2004) Ultrahigh-pressure corundum-rich garnetite in garnet peridotite, Sulu terrane, China. Contrib Mineral Petrol 147:21–31

Zhu Y (2003) Comments on ''Crystal-melt equilibria involving potassium-bearing clinopyroxene as indicator of mantle-derived ultrahigh-potassic liquid: an analytical review''. In: Perchuk LL, Safonov OG, Yapaskurt VO, Barton JM Jr (eds) [Lithos 60 (2002) 89–111] K-feldspar in metamorphic clinopyroxene, from exsolution to potassium replacement. Lithos 68:115–119